Supplement Materials for:

PGC-1β Deficiency Accelerates the Transition to Heart Failure in Pressure Overload Hypertrophy

Christian Riehle, MD[1]*, Adam R Wende, PhD[1]*, Vlad G Zaha, MD, PhD[1#], Karla Maria Pires, MS[1], Benjamin Wayment, MPH[2], Curtis Olsen, BS[1], Heiko Bugger, MD, PhD[1†], Jonathan Buchanan, MD[1], Xiaohui Wang, PhD[2], Annie Bello Moreira, PhD[1], Torsten Doenst, MD, PhD[5‡], Gema Medina-Gomez, PhD[4¶], Sheldon E Litwin, MD[2], Christopher J Lelliott, PhD[3], Antonio Vidal-Puig, MD, PhD[4], E. Dale Abel, MBBS, DPhil[1]

Detailed Methods

Mice and genotyping

All mouse experiments were approved by the Institutional Animal Care and Use Committee of the University of Utah. PGC-1β$^{-/-}$ germ-line KO mice (βKO) and wildtype littermate controls (WT) were generated and provided by the AstraZeneca Transgenics & Comparative Genomics Department, Mölndal, Sweden. βKO mice were generated using a triple LoxP targeting vector. Murine PGC-1β is alternatively spliced at the 5' end and at exon 4. Exons 4 and 5 were deleted, which encode for two of the nuclear hormone receptor interacting motifs (LXXLL). Ablation of exons 4 and 5 also introduced a premature stop codon. Following primers were used for genotyping: forward primer 1: 5'- GCACACCCGTGAATACTATGTA -3', reverse primer 1: 5'- CAAGGAGCAGGAACTGGGATT -3', and reverse primer 2: 5'- CCTTGGGCCTCCATCTCTGTT -3'.[1]

Composition of mouse chow

Mice were fed standard chow Harland Teklad Diet 8656 (3.8 Kcal/g of gross energy) that contained 65% carbohydrate (corn and soybean meal), 24.5 % protein (Soy based), 4.4 % fat (Soybean oil), 3.4 % fiber and supplemented with vitamins and minerals.

Surgical procedures and hemodynamic measurements (mouse experiments)

Aortic banding: Mice were anesthetized (single intraperitoneal injection of 400 mg chloral hydrate / kg body weight) and placed in the supine position on a heating pad (37 °C). A topical depilatory agent was applied to the chest, and the area was cleaned. Following horizontal skin incision ~ 0.5–1 cm in length at the level of the suprasternal notch, a 2- to 3-mm longitudinal cut was made in the proximal portion of the sternum. In our early studies a 6-0 silk suture was tightened around a blunt 27-G needle, which was placed between the innominate artery and the left common carotid artery. After ligation, the needle was quickly removed, and the chest and overlying skin were closed. We subsequently modified our protocol

to use a 27-G clip, as described in the Methods. The sham procedure was identical except that the aortic arch was not ligated.[2]

Cardiac Catheterization: Cardiac catheterizations with dobutamine infusion surgeries were performed as previously described [1, 3] with the following modifications. Mice at 7-wk of age were anesthetized (single intraperitoneal injection of 400 mg chloral hydrate / kg body weight) and placed in the supine position on a heating pad (37 °C). The left jugular vein was identified and accessed by cut down method using a 25 G needle connected to a 1 mL syringe with 80 ng/μL dobutamine hydrochloride that was mounted on a standard infuse/withdraw Harvard 33 twin syringe pump (Harvard Apparatus). A Millar Mikro-Tip catheter (1.0F; Millar Instruments, Houston TX) was then inserted into the left ventricle via the right carotid artery, and hemodynamic measurements were obtained using LabChart7 Pro software (ADInstruments, Colorado Springs, CO). After obtaining baseline pressure and heart rate recordings the dobutamine infusion was commenced with readings at 4, 8, 16, 32 and 64 ng/ g BW/ min infusion rates. Each dose was maintained for 1 min and the last 10 seconds of each dose were reported. Total volume infused was monitored to not exceed 75 μL per mouse over the entire procedure. In studies that were performed in sham and TAC mice at ages of 16-18 weeks (8-week banded cohort) or at 26-33 weeks (3-week banded cohort), the right carotid artery of anesthetized mice (chloral hydrate 400mg / kg body weight i.p.) was cannulated and a 1.4 F Millar Mikro-Tip catheter was used to obtain hemodynamic measurements.

Transthoracic echocardiography

Mice were anesthetized with isoflurane, placed supine and temperature was maintained with a heating pad (37 °C). Next, the chest hair was removed with a topical depilatory agent. Two-dimensional guided M-mode images were taken in short and long axis projections using a 13 MHz linear probe (Vivid FiVe, GE Medical Systems, Milwaukee, WI). Left ventricular dimensions and wall thickness were measured in at least three beats from each projection and averaged.[5, 6] Fractional shortening [%] was calculated as [(LVDd - LVDs) / LVDd] * 100 and ejection fraction [%] was calculated as [($LVDd^3$ - $LVDs^3$) / $LVDd^3$] * 100; where LVDd = left ventricular diastolic dimension and LVDs = left ventricular systolic dimension. In an apical long-axis view, pulsed wave Doppler recordings were made with the sample volume placed in the left ventricular outflow tract (LVOT). Stroke volume [μl] was calculated as π * (LVOT diameter/2)^2 * LVOT VTI; where VTI = the velocity time integral [cm]. Cardiac output was calculated as SV * HR; where SV = stroke volume [μl] and HR = heart rate [beats/min].

Measurement of carotid velocity gradients

It is difficult to noninvasively measure the gradient across a band placed on the transverse aortic arch in mice. Therefore, we measured flow velocity in the right and left carotid arteries of sham and banded mice using pulsed wave Doppler. A 13 MHz Doppler probe was used to measure flow velocity both in the right carotid artery proximal to the aortic constriction and in the left carotid artery distal to the aortic constriction immediately after surgery. The peak flow velocity difference of the right / left carotid artery was used to determine the transaortic gradient.[4] The peak flow velocities in the right and left carotid arteries in sham-operated animals were (mean±SEM) 0.46±0.021 and 0.435±0.021 m/s, respectively, $p>0.35$, n= 11). In contrast, following application of a 27 gauge clip to the aortic arch between the right inominate artery and the left carotid artery, the flow velocities in the right and left carotid arteries were 0.63±0.038 and 0.359 ±0.038 m/s, $p<0.0001$, n=8). Increased flow in the vessel proximal to the clip and decreased flow distal is consistent with significant narrowing of the aorta.

Mitochondrial Function Measurements – Overview

Left ventricular muscle fibers were dissected from freshly excised hearts and permeabilized with saponin. Respiration and ATP synthesis were measured using palmitoyl-carnitine (20µM, PC), pyruvate (10mM, Pyr) as substrates, each combined with malate (2mM). Oxygen consumption was determined under three different conditions: in the presence of substrate alone (V_0), following ADP-stimulation (1mM; V_{ADP}) and after addition of the ATP synthase inhibitor oligomycin (1µg/ml; V_{Oligo}).

Saponin-permeabilized cardiac fibers

Mitochondrial function was measured in saponin-permeabilized cardiac muscle fibers.[7] Small pieces (2 to 5 mg) of left ventricular cardiac muscle were dissected from freshly excised hearts and permeabilized for 30 minutes at 4 °C in buffer A (50 µg/mL saponin, 7.23 mmol/L K_2EGTA, 2.77 mmol/L K_2CaEGTA, 6.56 mmol/L $MgCl_2$, 20 mmol/L imidazole, 0.5 mmol/L dithiothreitol, 53.3 mmol/L K-methanS, 20 mmol/L taurine, 5.3 mmol/L Na_2ATP, 15 mmol/L PCr, and 3 mmol/L KH_2PO_4, pH 7.1 adjusted at 25 °C). Next, fibers were washed twice for 10 minutes at 4 °C in buffer B (7.23 mmol/L K_2EGTA, 2.77 mmol/L K_2CaEGTA, 1.38 mmol/L $MgCl_2$, 20 mmol/L imidazole, 0.5 mmol/L dithiothreitol, 100 mmol/L K-methanS, 20 mmol/L taurine, 3 mmol/L KH_2PO_4, 2 mg/mL BSA, 2 mmol/L malate, and 20 µmol/L Palmitoyl-carnitine or 10 mmol/L pyruvate as substrate, pH 7.1 adjusted at 25 °C).

Mitochondrial oxygen consumption

The respiratory rates of cardiac fibers were measured using a oxygen sensor probe (Ocean Optics, Dunedin, FL) in 2 ml of KCl buffer at 25 °C (125 mmol/L KCl, 20 mmol/L HEPES, 3 mmol/L Mg-Acetate, 0.4 mmol/L EGTA, 2 mg/ml BSA, 5 mmol/L KH_2PO_4 and 0.3 mmol/L Dithiothreitol, 2 mmol/L

malate, and 20 µmol/L Palmitoyl-carnitine or 10 mmol/L pyruvate as substrate, pH 7.1 adjusted at 25 °C). Oxygen consumption was determined under three different conditions: in the presence of substrate alone (V_0), following ADP-stimulation (1mM; V_{ADP}) and after addition of the ATP synthase inhibitor oligomycin (1µg/ml; V_{Oligo}). The solubility of oxygen in KCl buffer was 246.87 nmol of O_2 / mL. Oxygen consumption rates were expressed as nmol of O_2 * min^{-1} * mg dry fiber $weight^{-1}$.

Mitochondrial ATP production

For measurement of ATP production, ADP was added to 2 ml of buffer B to a final concentration of 1 mmol/L. Next, 10 µl Buffer B from the respiration chamber were added to 190 µl DMSO every 10 seconds for a 1-min time period. ATP production was determined by a bioluminescence assay based on the luciferin/luciferase reaction with the ATP assay kit (Promega Corporation, Madison, WI).

Isolated working mouse hearts

Hearts were perfused in the isolated working heart mode with Krebs Henseleit Buffer (118.5 mmol/L NaCl, 25 mmol/L NaHCO3, 4.7 mmol/L KCl, 1.2 mmol/L MgSO4, 1.2 mmol/L KH2PO4, 2.5 mmol/L CaCl2, 0.5 mmol/L EDTA, and 5 mmol/L glucose, gassed with 95% O_2 and 5% CO_2 and supplemented with 0.4 mmol/L palmitate bound to 3% BSA) using a perfusion apparatus totally sealed to prevent loss of CO_2. Throughout the 60-min perfusion, measurements of flow and pressure (Millar pressure catheter, Millar Instruments, Houston, TX) were obtained every 20-min. Using a fiber-optic oxygen sensor (Ocean Optics, Orlando, FL), the oxygen content of freshly oxygenated buffer (arterial partial pressure of oxygen [PaO_2]) and oxygen concentration in pulmonary artery effluent, collected using a capillary tube (venous partial pressure of oxygen [PvO_2]) was measured.

Palmitate oxidation was measured in one set of hearts and glycolytic flux and glucose oxidation rates were measured simultaneously in a second set of hearts. Glucose oxidation was assessed by measuring $^{14}CO_2$ released by the metabolism of [U-^{14}C] glucose (specific activity = 296 Mbq/mol). The amount of ^3H_2O released from the metabolism of exogenous [5-^{3}H] glucose (specific activity = 177 Mbq/mol) was used to determine glycolytic flux. Palmitate oxidation rates were measured by determining the amount of ^3H_2O released from [9,10-^{3}H] palmitate (specific activity = 42 Gbq/mol).[8]

The following formulas were used to determine myocardial oxygen consumption, cardiac hydraulic work and cardiac efficiency:

MVO_2 [ml * min^{-1} * g^{-1} WHW] = [(PaO_2-PvO_2)/100) * (Coronary flow/WHW) * (725/760) * (1000 * C)]; where PaO_2 = arterial partial pressure of oxygen [mmHg], PvO_2 = venous partial pressure of oxygen [mmHg], WHW = wet heart weight [g], 725 and 760 are atmospheric pressures at the University of Utah and at sea level respectively [mmHg], and C = Bunsen Coefficient for plasma i.e. 0.0212.

Cardiac hydraulic work [J * min^{-1} * g^{-1} WHW] = CO * DevP * 1.33 * 10^{-4} / g WHW; where CO = Cardiac output [ml/min], and DevP = Developed pressure [mm Hg].

Cardiac efficiency [%] = Hydraulic work / MVO_2 * 100. $MV0_2$ [ml/min] was converted to µmol/min by multiplying by the conversion factor 0.0393, and then to Joules [J/min] using the conversion of 1µmol 0_2 = 0.4478 J as previously described.[9]

Measurement ROS levels

A fluorometric assay based on the conversion of non-fluorescent 2', 7'-dichlorofluorescein-diacetate (DCFDA) to the highly fluorescent DCF in the presence of ROS was used to measure ROS levels in heart homogenates. Following homogenization in homogenization buffer (1 mM EDTA, 50 mM phosphate buffer, 1 tablet Phosphatase Inhibitor Cocktail 1 and 2 (Sigma-Aldrich, St. Louis, MO) 1 tablet Complete Mini Protease Inhibitor Cocktail (Roche, Nutley, NJ), pH 7.4) samples were centrifuged at 900 g for 15 min. Next, the supernatant was centrifuged at 12,000 g for 15 min. The oxidation-sensitive carboxy-H_2DCFDA (C400, Molecular Probes, Carlsbad, CA) or the oxidation-insensitive carboxy-DCFDA (C369, Molecular Probes) were added to 100 µg of supernatant protein with 25 µM final concentration at 37 °C. The change in fluorescence intensity was measured at 0 and 30 min using a fluorescence plate reader (485 nm excitation/530 nm emission). Data were expressed as C400 / C369 ratios and results were compared to sham operated wildtype mice.[10]

Immunoblotting analysis

For immunoblotting analysis, ~ 50 mg of frozen tissue was homogenized in 100 µl Lysis buffer (50 mmol/L Hepes, 150 mmol/L NaCl, 10% Glycerol, 1% Triton X-100, 1.5 mmol/L MgCl2, 1 mmol/L EGTA, 10 mmol/L Sodium Pyrophosphate, 100 mmol/L Sodium Fluoride and 100 µmol/L Sodium Vanadate, 1 mmol/L PMSF, 10 µg/ml Aprotinin, and 10 µg/ml Leupeptin) using a motor-driven tissue homogenizer. Tissue lysates were resolved on SDS-PAGE and transferred to PVDF membranes (Millipore Corp., Billerica, MA). Primary and secondary antibodies used are summarized in the table below.

Antigen	**Company**	**Catalog #**	**~Size (kDa)**	**2°**
Phospho-AMPKa (Thr172)	Cell Signaling, Danvers, MA	CS-2531	**62**	Rabbit
AMPKa	Cell Signaling	CS-2793	**62**	Mouse
GAPDH	Cell Signaling	CS-2118	**37**	Rabbit
GLUT4	Millipore, Billerica MA	MP 04-1404	**50**	Mouse

HKII (hexokinase)	Chemicon, Temecula CA	AB3279	**102**	Rabbit
MnSOD	BD Biosciences, San Jose CA	BD-611580	**25**	Mouse
Phospho-PDH (Ser293)	Calbiochem, San Diego CA	AP1062	**44**	Rabbit
Pyruvate dehydrogenase E1-a	Abcam, Cambridge MA	ab67592	**43-50**	Mouse
a-Tubulin	Sigma Aldrich, St. Louis MO	S-T5168	**50**	Mouse
UCP3	ABR Affinity BioReagents, Golden CO	ABR PA1-055	**32**	Rabbit
VDAC	ABR Affinity BioReagents	ABR PA1-954	**32**	Rabbit
Anti-Rabbit-AlexaFluor 680	Invitrogen, Carlsbad CA	Invitrogen A21109		
Anti-Mouse IRDYE800	Li-COR, Lincoln NE	Li-Cor 926-32212		

IRDye 800CW anti-Mouse (LICOR, Lincoln, NE) and Alexa fluor anti-Rabbit 680 (Invitrogen, Carlsbad, CA) were used as secondary antibodies and fluorescence was quantified using the LICOR Odyssey imager.

RNA extraction and quantitative RT-PCR (mouse experiments)

Total RNA was extracted from hearts with TRIzol reagent (Invitrogen Corporation, Carlsbad, CA) and purified with the RNAeasy kit (Qiagen Inc., Valencia, CA). RNA concentration was determined by measuring the absorbance at 260 nm and 280 nm using a spectrophotometer (NanoDrop 1000, NanoDrop products, Wilmington, DE). Total RNA (~ 3 µg) was reverse transcribed (SuperScriptTM III Reverse Transcriptase Kit, Invitrogen, Carlsbad, CA). The resulting cDNA, Platinum Taq DNA polymerase (Invitrogen), primers, and SYBR-green (Invitrogen) fluorescent dye were transferred to a 384-well plate in triplicate and real-time polymerase chain reaction was performed with an ABI Prism 7900HT instrument (Applied Biosystems, Foster City, CA). The following cycle profile was used: 1 cycle at 95 °C for 10 min, 40 cycles of 95 °C for 15 sec, 59 °C for 15 sec, 72 °C for 30 sec, and 78 °C for 10 sec, 1 cycle of 95 °C for 15 sec, 1 cycle of 60 °C for 15 sec, and 1 cycle of 95 °C for 15 sec. Data were normalized to Cyclophilin and results were compared to sham operated wildtype mice. See online-only Data Supplement Table S3 for primer sequences.

Electron Microscopy

Left ventricular samples were fixed in 2.5 % glutaraldehyde and 1 % paraformaldehyde for at least 1 day. Samples were post-fixed in 2 % osmium, stained en bloc with aqueous uranyl acetate, and dehydrated

through a graded series of ethanol washes (50% up to 100%). Next, samples were embedded in Spurr's plastic and processed for electron microscopy.[11] Mitochondrial morphology was assessed at 10,000 x and 40,000 x magnifications. Mitochondrial number and volume density were assessed in a blinded fashion using the point quantification counting.[12] For volume density, 2 pictures per sample were analyzed using 2 grids per picture. For mitochondrial number, 3 pictures per sample were analyzed.

Histology and Stereology:

Myocardial fragments were stained by hematoxylin-eosin, Masson's trichrome, TUNEL, and DAPI stains. Light microscopy was performed using an Olympus LX81 inverted microscope that was connected to an Olympus Microfire Digital Camera (New York, NY). In the 3 µm-thick sections, myocardium was analyzed with a 36-point test-system. From each sample, ten microscopic fields were analyzed at random by the same observer, the stage of the microscope being moved blindly. Volume density was estimated for cardiomyocytes (cmy) and interstitium (int): ($Vv[structure] := P_p[structure]/P_T$) ($P_p$ is the number of points that hit the structure; P_T is the total test-points inside the frame). The mean cross-sectional area was estimated for cardiomyocytes, $A[cmy] := Vv[cmy]/2$. $N[cmy] \cdot A_T^{-1}$ (μm^2; $1/mm^2$, N is the number of profiles counted in the test-area, the frame A_T, considering the forbidden line or its extensions). The absolute stereological indices of interstitial volume was estimated by the product of Vv[int] and the respective cardiac volume.[12]

Surgical procedures (rat experiments)

Male Sprague-Dawley rats (380 – 430 g) were obtained from Charles River (Sulzfeld, Germany). The use of animals and the experimental protocol were approved by the German Animal Welfare Committee of Baden-Wuerttemberg, Freiburg jurisdiction. Rats were operated in an analogous manner as described for mice (anaesthesia: 50 mg ketamine / kg body weight and 10 mg xylazine / kg body weight). A 3-0 silk suture was tightened around a blunt 20-G needle, which was placed between the innominate artery and the left common carotid artery. The sham procedure was identical except that the aortic arch was not ligated. The rats were sacrificed two weeks after surgery.

RNA extraction and quantitative RT-PCR (rat experiments)

RNA extraction, RNA purification and determination of RNA concentration (spectrophotometer Ultrospec 2100 pro, Amersham Pharmacia Biotech) were performed as described for mouse experiments. The resulting cDNA, primers, probes, and LightCycler® 480 Probes Master Mix (Roche Applied Science, Mannheim, Germany) were transferred to a 384-well plate in triplicate and real-time polymerase chain reaction was performed with a LightCycler® 480 instrument (Roche Applied Science, Mannheim,

Germany). The following cycle profile was used: 1 cycle at 95 °C for 5 min, 45 cycles of 95 °C for 10 sec, 60 °C for 30 sec, 72 °C for 30 sec, 1 cycle at 40 °C for 5 min. Data were normalized to S29 and results were compared to sham operated rats. See online-only Data Supplement Table S6 for primer and probe sequences.

Statistical analysis

All results are expressed as means ± SEM. Unpaired Student's t tests were used to determine p-values when comparing two groups. For multi-group comparisons, differences were analyzed by ANOVA, and significance was assessed by Fisher's protected least significant difference test. Data that were non-normally distributed were analyzed by the non-parametric Wilcoxon Rank Sums test. Analysis of covariance (ANCOVA) was used to evaluate the effect of genotype and dobutamine infusion for cardiac catheterization studies. Statistical calculations were performed using the StatView 5.0.1 or JMP software packages (SAS Institute, Cary, NC). Differences were considered statistically significant for p-values < 0.05.

Supplemental Online Figures

Online Figure I

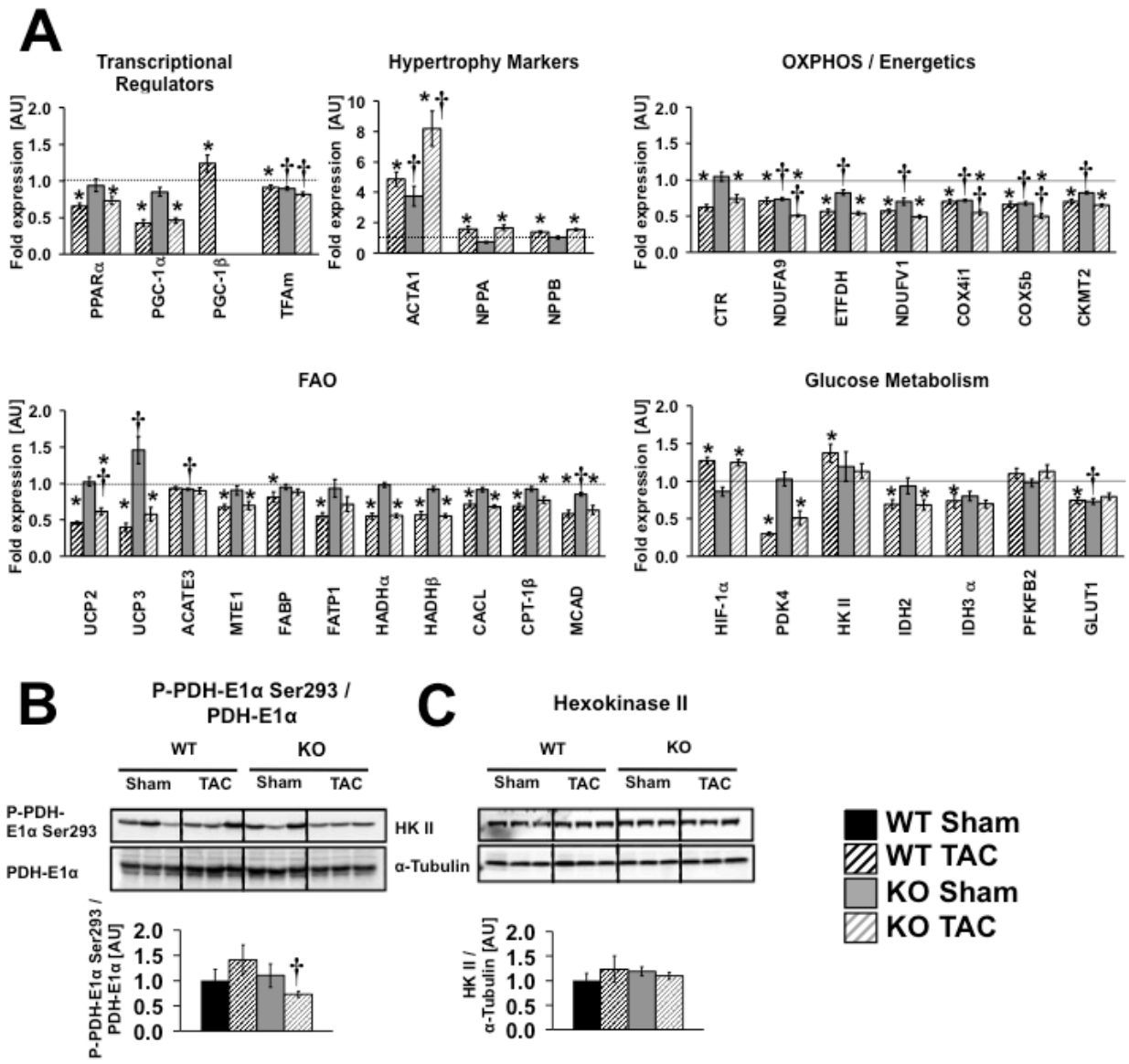

Online Figure I:
Representative longitudinal electron microscopy images of left ventricular wall eight weeks after Sham or TAC surgery (A). For mitochondrial number (B) and mitochondrial volume density (C) no significant difference was observed between the groups. Data were obtained from 4 hearts per group.

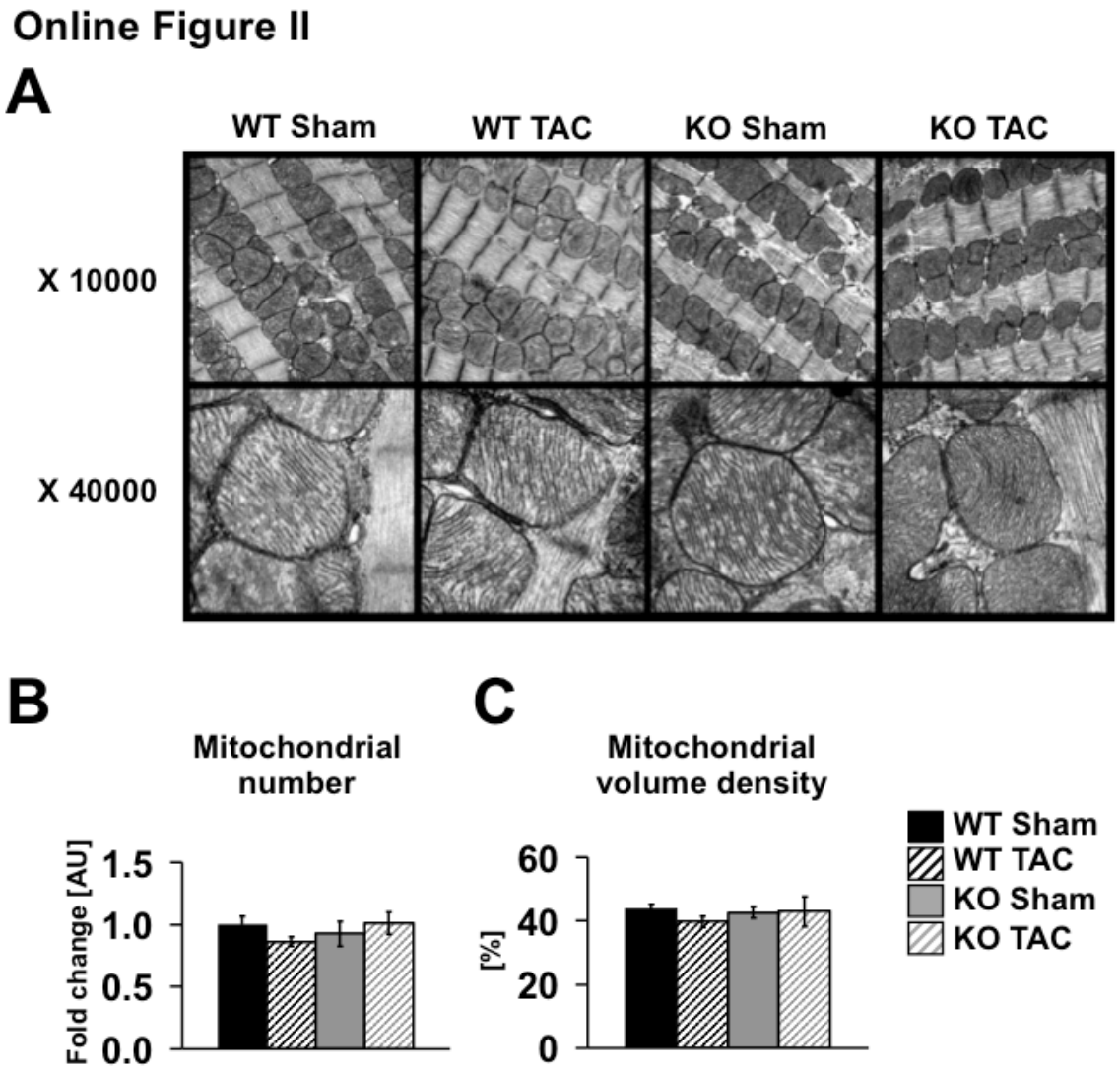

Online Figure II:
(A) Gene expression three weeks post surgery (n =8). (B, C) Western blot analysis and densitometric ratios of PDH-E1α phosphorylation and Hexokinase II protein expression in WT and KO hearts three weeks after surgery (n = 5-6). * = $p<0.05$ vs. Sham same genotype, † = $p<0.05$ vs. WT same treatment. Gene names are shown in Online Table III.

Supplemental Online Tables

Online Table I: Primer Sequences used for Quantification of mRNA and DNA levels by RT-PCR (mouse)

Gene Name
Gene Sequence of forward and reverse primers (5'→3')
GenBank Accession Number

6-phosphofructo-2-kinase/fructose-2,6-biphosphatase 2 (PFKFB2)
CGGGAATGGATCTACACTGG
GGAGAGCAAAGTGAGGGATG
NM_008825

Actin, alpha 1, skeletal muscle (ACTA1)
CCTGTATGCCAACAACGTCA
CTCGTCGTACTCCTGCTTGG
XM_134551

Acyl-CoA thioesterase 10 (Acate3)
CAGAAGCCTGTTGAAGTTGGT
GACTTGAAATGTCGCTGTCC
NM_022816.2

ATPase, Ca++ transporting, cardiac muscle, slow twitch 2 (Atp2a2)
TGGGAGAATATCTGGCTCGT
AGTCGGGTTGTTCCAGGTAG
NM_001110140

Calcium channel, voltage-dependent, L type, alpha 1C subunit (Cacna1c)
AAGAGGGAGATCCAGCCATC
TGGGGAATGTGGTAGGAGAA
NM_001159535

Carnitine palmitoyltransferase 1 beta – muscle (CPT1β)
TGCCTTTACATCGTCTCCAA
AGACCCCGTAGCCATCATC
NM_009948

Citrate synthase (CS)
CTCACAGTGGGGTGCTGCT
CCCAGTCTCCCATTTTACCC
NM_026444

Creatine kinase, mitochondrial 2 (CKMT2)
AGAACTGCGGCTCCAAAAG
CACTTCCTGCCAAACTGAGG
NM_198415.2

Cyclophilin A (CPHN)
AGCACTGGAGAGAAAGGATTTGG

TCTTCTTGCTGGTCTTGCCATT
NM_008907

Cytochrome c oxidase subunit IV isoform 1 (Cox4i1)
CGCTGAAGGAGAAGGAGAAG
GCAGTGAAGCCAATGAAGAA
NM_009941

Cytochrome c oxidase, subunit Vb (Cox5b)
TGGAGGTGGTGTCCCTACTG
CTCTTGTTGCTGATGGATGG
M_009942
Electron transferring flavoprotein, dehydrogenase (ETFDH)
CCTCTGTGGCTTTGAGTGGT
TCGAAATCCATCACCTTGTTC
NM_025794

Fatty acid binding protein 3 (FABP)
GACGGGAAACTCATCCTGAC
TCTCCAGAAAAATCCCAACC
NM_010174.1

Hexokinase II (HK II)
CCTTGGATCTTGGAGGAACA
CAAGGGAAGGAGAAGGTGAA
NM_013820.3

Hydroxyacyl-CoA Dehydrogenase - alpha subunit (HADHα)
TCAGGAGGGCTCAAAGAATAA
GAAAGCCAAGCCCAAAGAC
XM_131963

Hydroxyacyl-CoA Dehydrogenase - beta subunit (HADHβ)
GCCAACAGACTGAGGAAGGA
ACACTGGCAAGGCTGGATT
NM_145558

Hypoxia inducible factor 1, alpha subunit (HIF-1α)
TCACCAGACAGAGCAGGAAA
CTTGAAAAAGGGAGCCATCA
NM_010431

Isocitrate dehydrogenase 2 (NADP+), mitochondrial (IDH2)
CCCTATTGCCAGCATCTTTG
TGTCCAGGAAGTCTGTGGTG
NM_173011

Isocitrate dehydrogenase 3 (NAD+) alpha (IDH3α)
CCCATCCCAGTTTGATGTTC
GCATCATCACAGCACTAAGCA
NM_029573

Medium chain acetyl-Coenzyme A dehydrogenase (MCAD)
ACTGACGCCGTTCAGATTTT
GCTTAGTTACACGAGGGTGATG
NM_007382

Mitochondrial acyl-CoA thioesterase 1 (MTE1)
GACCTCCCCAAGAGCATAGA
TCCTTGTAGGAGATGGTGTTCC
NM_134188

NADH dehydrogenase (ubiquinone) 1 alpha subcomplex 9 (Ndufa9)
ATCCCTTACCCTTTGCCACT
CCGTAGCACCTCAATGGACT
NM_025358

NADH dehydrogenase (ubiquinone) flavoprotein 1 (Ndufv1)
TGTGAGACCGTGCTAATGGA
CATCTCCCTTCACAAATCGG
NM_133666

Natriuretic peptide precursor type A (NPPA)
ATGGGCTCCTTCTCCATCA
CCTGCTTCCTCAGTCTGCTC
K02781

Natriuretic peptide precursor type B (NPPB)
GGATCTCCTGAAGGTGCTGT
TTCTTTTGTGAGGCCTTGGT
D16497

Peroxisome proliferator activated receptor alpha (PPAR-α)
GAGAATCCACGAAGCCTACC
AATCGGACCTCTGCCTCTTT
NM_011144

Peroxisome proliferator activated receptor gamma co-activator 1 alpha (PGC-1α)
GTAAATCTGCGGGATGATGG
AGCAGGGTCAAAATCGTCTG
NM_008904

Peroxisome proliferator activated receptor gamma co-activator 1 beta (PGC-1β)
TGAGGTGTTCGGTGAGATTG
CCATAGCTCAGGTGGAAGGA
NM_133249

Pyruvate dehydrogenase E1 alpha 1 (PDHA1)
GGGACGTCTGTTGAGAGAGC
TGTGTCCATGGTAGCGGTAA
NM_008810.2

Pyruvate dehydrogenase kinase 4 (PDK4)
GCTTGCCAATTTCTCGTCTC
CTTCTCCTTCGCCAGGTTCT
NM_013743

Solute carrier family 2 (facilitated glucose transporter), member 1 (GLUT1)
GTCCTGCTCGTATTGCTGTG
GCCTTTGGTCTCAGGGACTT
NM_011400

Solute carrier family 25 (mitochondrial carnitine/acylcarnitine translocase), member 20 (CACL)
CCTGCCAGTGGGATGTATTT
TCGGATCAGCTCTCTCAACA
NM_020520

Solute carrier family 27 (fatty acid transporter), member 1 (FATP1)
CCATCTTCCTGCGTCTTCTG
GTGTCAGGCTCCCAGGTCTC
NM_011977.3

Solute carrier family 6 (neurotransmitter transporter, creatine), member 8 (CTR)
TGATGTGAGTGGGGGTAAGG
AGGACCAGCACCATTTCATC
NM_133987

Transcription factor A, mitochondrial (TFAm)
CAAAAAGACCTCGTTCAGCA
CTTCAGCCATCTGCTCTTCC
NM_009360

Uncoupling protein 2 (UCP2)
TCTCCTGAAAGCCAACCTCA
CTACGTTCCAGGATCCCAAG
NM_011671.4

Uncoupling protein 3 (UCP3)
TTTGGAGCTGGCTTCTGTG
AAGGCCCTCTTCAGTTGCTC
NM_009464.3

Primer pairs were designed based on GenBank reference sequences. We used the WWW interface Primer 3 (http://frodo.wi.mit.edu/cgi-bin/primer3/primer3_www.cgi) with default settings. To avoid non-specific amplifications, primer sequences were blasted against mouse genes. Dissociation curves were analyzed for all primer-pairs to ensure single product amplification.

Online Table II: Weights of WT and KO hearts 8 weeks after TAC or sham surgery

Group (n)	BW [g]	HW [mg]	TL [mm]	HW / BW [mg/g]	HW / TL [mg/mm]
WT Sham (12)	28.8 ± 0.7	141.7 ± 2.4	17.20 ± 0.08	4.93 ± 0.10	8.24 ± 0.13
WT TAC (12)	29.0 ± 0.8	255.0 ± 21.9*	17.28 ± 0.10	8.91 ± 0.91*	14.73 ± 1.23*
KO Sham (12)	27.9 ± 0.7	142.3 ± 5.1	16.75 ± 0.10 †	5.11 ± 0.17	8.49 ± 0.29
KO TAC (12)	27.2 ± 1.0	270.8 ± 17.0*	16.75 ± 0.13 †	10.29 ± 0.98*	16.16 ± 0.98*

BW, Body weight; HW, Heart weight; TL, Tibia length; HW / BW, Heart weight/Body weight ratio; HW / TL, Heart weight/Tibia length ratio
* = $p<0.05$ vs. Sham same Genotype; † = $p<0.05$ vs. WT same Treatment

Online Table III: Cardiac Function by Echocardiography in WT and PGC-1β$^{-/-}$ 8 weeks following TAC or Sham Surgery

Time after surgery [wk]	Group (n)	LVDd [mm]	LVDs [mm]	IVSd [mm]	LVPWd [mm]	FS [%]	EF [%]	SV [µl]	HR [bpm]	CO [ml/min]
0	WT Sham (8)	4.05 ± 0.13	2.64 ± 0.16	0.99 ± 0.07	0.96 ± 0.08	35.4 ± 2.3	72.3 ± 2.8	28 ± 1	456 ± 14	12.9 ± 0.3
	WT TAC (13)	4.16 ± 0.11	2.66 ± 0.12	1.04 ± 0.04	1.01 ± 0.07	36.4 ± 1.9	73.3 ± 2.4	31 ± 1	458 ± 12	14.4 ± 0.7
	KO Sham (9)	4.22 ± 0.09	2.64 ± 0.08	1.04 ± 0.05	1.10 ± 0.04	37.1 ± 1.1	74.9 ± 1.3	30 ± 1	435 ± 14	12.9 ± 0.5
	KO TAC (10)	4.34 ± 0.16	2.80 ± 0.15	1.08 ± 0.06	1.01 ± 0.07	36.0 ± 1.7	72.9 ± 1.8	33 ± 2	447 ± 16	14.6 ± 1.1
1	WT Sham (8)	3.60 ± 0.12	2.35 ± 0.16	1.03 ± 0.06	1.11 ± 0.08	35.4 ± 2.3	72.6 ± 2.6	26 ± 2	497 ± 16	13.0 ± 1.0
	WT TAC (13)	4.08 ± 0.15*	2.72 ± 0.19	1.13 ± 0.05	1.17 ± 0.06	34.0 ± 2.5	69.8 ± 3.1	23 ± 2	520 ± 19	12.0 ± 0.9
	KO Sham(9)	4.20 ± 0.14†	2.70 ± 0.17	1.07 ± 0.07	1.02 ± 0.07	36.2 ± 2.9	72.8 ± 3.5	28 ± 1	460 ± 12	13.1 ± 0.8
	KO TAC (9)	3.77 ± 0.15	2.24 ± 0.21	1.27 ± 0.09*	1.30 ± 0.12*	41.5 ± 3.8	78.1 ± 3.5	23 ± 2*	532 ± 14*	12.2 ± 0.9
2	WT Sham (8)	3.75 ± 0.16	2.20 ± 0.18	0.96 ± 0.05	0.96 ± 0.08	41.5 ± 3.6	78.3 ± 3.7	30 ± 1	479 ± 12	14.5 ± 0.6
	WT TAC (13)	4.23 ± 0.10	2.89 ± 0.11*	1.12 ± 0.04	1.24 ± 0.06*	31.4 ± 1.5*	67.3 ± 2.0*	23 ± 1*	494 ± 14	11.4 ± 0.5*
	KO Sham (9)	4.19 ± 0.14	2.72 ± 0.21	1.01 ± 0.07	0.94 ± 0.06	37.0 ± 1.7	75.0 ± 2.4	28 ± 2	467 ± 8	12.9 ± 0.9
	KO TAC (9)	4.57 ± 0.32	3.03 ± 0.33	1.19 ± 0.08	1.16 ± 0.07*	34.7 ± 3.0	70.6 ± 4.2	23 ± 2*	490 ± 22	11.1 ± 0.6
3	WT Sham (8)	3.75 ± 0.17	2.31 ± 0.18	0.98 ± 0.04	0.93 ± 0.05	39.1 ± 2.5	76.8 ± 2.7	25 ± 2	468 ± 5	11.8 ± 0.8
	WT TAC (13)	4.37 ± 0.19*	2.95 ± 0.25	1.18 ± 0.04*	1.11 ± 0.05*	33.7 ± 3.2	68.5 ± 4.0	27 ± 2	484 ± 11	13.1 ± 0.9
	KO Sham (9)	4.04 ± 0.20	2.53 ± 0.19	1.06 ± 0.06	1.01 ± 0.06	37.7 ± 2.8	74.7 ± 2.6	27 ± 2	460 ± 13	12.3 ± 1.2
	KO TAC (9)	4.59 ± 0.24	3.23 ± 0.26	1.06 ± 0.05	1.13 ± 0.04	30.0 ± 2.2	65.0 ± 3.1	25 ± 2	451 ± 23	10.9 ± 0.6
8	WT Sham (11)	4.48 ± 0.05	3.43 ± 0.06	0.62 ± 0.02	0.64 ± 0.02	24.3 ± 1.0	55.1 ± 1.7	49 ± 1	422 ± 23	20.7 ± 1.4
	WT TAC (10)	5.03 ± 0.19*	4.33 ± 0.25*	0.76 ± 0.06*	0.79 ± 0.05*	17.9 ± 2.5*	41.6 ± 4.1*	48 ± 5	470 ± 22	22.3 ± 2.3
	KO Sham (11)	4.37 ± 0.10	3.31 ± 0.12	0.69 ± 0.04	0.67 ± 0.03	24.4 ± 1.1	56.6 ± 1.9	45 ± 2	474 ± 24	21.3 ± 1.3
	KO TAC (9)	5.62 ± 0.19*†	5.01 ± 0.22*†	0.66 ± 0.02	0.81 ± 0.05*	11.1 ± 1.1*†	29.6 ± 2.6*†	41 ± 4	435 ± 18	18.0 ± 2.4

LVDd, Left ventricular cavity diameter at diastole; LVDs, Left ventricular cavity diameter at systole; IVSd, Interventricular septum diameter at diastole; LVPWd, Left ventricular posterior wall thickness at diastole; FS, Fractional shortening; EF, Ejection fraction; SV, Stroke volume; HR, heart rate; CO, Cardiac output;

* = $p<0.05$ vs. Sham same Genotype; † = $p<0.05$ vs. WT same Treatment

Online Table IV: Weights of rat hearts 2 weeks after TAC or sham surgery

Group (n)	BW [g]	HW [g]	HW / BW [mg/g]
Sham (8)	437 ± 22	1.13 ± 0,08	2.59 ± 0.26
TAC (8)	411 ± 27	1.24 ± 0,10*	3.03 ± 0.22*

BW, Body weight; HW, Heart weight; HW / BW, Heart weight/Body weight ratio;
* = $p<0.05$ vs. Sham

Online Table V: Gene expression in rat hearts 2 weeks following TAC

	Sham	**TAC**	
Transcriptional regulators			
PGC-1α	1.00 ± 0.09	0.60 ± 0.04	*
PGC-1ß	1.00 ± 0.09	0.65 ± 0.03	*
PPAR-α	1.00 ± 0.07	0.80 ± 0.07	p = 0.0504 vs. Sham
ERRα	1.00 ± 0.07	0.71 ± 0.11	*
NRF1	1.00 ± 0.25	1.10 ± 0.24	
NRF2a	1.00 ± 0.08	0.95 ± 0.07	
TFAm	1.00 ± 0.12	0.92 ± 0.05	
Polr2a	1.00 ± 0.08	0.84 ± 0.06	
Hypertrophy markers / cardiac structure			
NPPA	1.00 ± 0.28	2.81 ± 0.42	*
αMHC	1.00 ± 0.09	0.66 ± 0.06	*
ßMHC	1.00 ± 0.12	0.95 ± 0.09	
OXPHOS			
Ndufa10	1.00 ± 0.07	0.89 ± 0.07	
Sdhb	1.00 ± 0.08	0.72 ± 0.05	*
Uqcrc2	1.00 ± 0.06	0.90 ± 0.04	
Cox4i1	1.00 ± 0.07	0.84 ± 0.06	
Atp2a2	1.00 ± 0.05	0.81 ± 0.05	*
FAO			
LCAD	1.00 ± 0.05	0.80 ± 0.06	*

MCAD	1.00 ± 0.18	0.57 ± 0.07	*
CPT1ß	1.00 ± 0.04	0.80 ± 0.09	p = 0.066 vs. Sham
FABP	1.00 ± 0.04	0.74 ± 0.07	*
FAT	1.00 ± 0.06	0.81 ± 0.08	p = 0.078 vs. Sham
Glucose metabolism			
PDHE1α	1.00 ± 0.05	0.93 ± 0.06	
PDP1	1.00 ± 0.26	0.61 ± 0.05	
PDK4	1.00 ± 0.16	1.71 ± 0.12	*
GLUT1	1.00 ± 0.12	1.04 ± 0.18	
GLUT4	1.00 ± 0.07	0.78 ± 0.05	*
GSK-3ß	1.00 ± 0.06	0.95 ± 0.13	
HIF-1α	1.00 ± 0.06	0.80 ± 0.08	p = 0.079 vs. Sham
HK2	1.00 ± 0.11	0.93 ± 0.09	

n =8, * = $p<0.05$ vs. Sham surgery, gene names are shown in supplementary table S6.

Online Table VI: Primer Sequences used for Quantification of mRNA and DNA levels by RT-PCR (rat)

Gene Name
Gene Sequence of forward and reverse primers and probes (5'→3')
GenBank Accession Number

ATPase, Ca++ transporting, slow twitch 2 (Atp2a2)
CTGGAAGATTCTGCGAACTTCA
CCCACACAGCCAACGAAAG
6-FAM-CAAATATGAGACCAATCTG-MGB
NM_017290

Carnitine palmitoyltransferase 1 beta – muscle (CPT1β)
AGTGTGCCAGCCACAATTCA
ATAGGCTTCGTCATCCAGCAA
6-FAM-CGGTACTTGGATTCTGTGC-MGB
NM_013200

Cytochrome c oxidase subunit IV isoform 1 (Cox4i1)
GCCTTTCCAGGGATGAGAAAG
TCTCAGCGAAGCTCTCGTTAAA
6-FAM-CCAATTGTACCGCATCC-MGB
NM_017202

Estrogen related receptor, alpha (ERRα)
CCTGGTCTGTGGGGATGT
GGACAGCTGTACTCGATGCTC
#106 *
NM_001008511

Fatty acid binding protein 3 (FABP)
TTTGTCGGTACCTGGAAGCTA
CACCTGTCTGGTGGCAAAG
#56 *
AF144090

Fatty acid translocase (FAT)
TTACTGGAGCCGTTATTGGTG
TCCTTCTTCAAGGACAACTTCC
#76 *
NM_001109218

Glycogen synthase kinase 3 beta (GSK-3ß)
CAGCTTTTGGTAGCATGAAAGTT
CAGGAGTTGCCACCACTGT
#121*
NM_032080

Hexokinase II (HK II)
CCAGCAGAACAGCCTAGACC
AGATGCCTTGAATCCCTTTG
#101 *
NM_012735

Hypoxia inducible factor 1, alpha subunit (HIF-1α)
CAGAGGAAGCGAAAAATGGA

TTGCTGCAGTAACGTTCCAA
#18 *
NM_024359

Long chain acetyl-Coenzyme A dehydrogenase (LCAD)
GCAGTTACTTGGGAAGAGCAA
GGCATGACAATATCTGAATGGA
#81 *
NM_012819

Medium chain acetyl-Coenzyme A dehydrogenase (MCAD)
GGGACTAGGGTTTAGCTTCGAG
CCGAGCAATTGTTTGAAACTC
#84 *
NM_016986

Myosin, heavy chain 6, cardiac muscle, alpha (αMHC))
CAGAAGAAACTGAAGGAAAACCA
GCTCCGCCTCTAGCTCCT
#17 *
NM_017239

Myosin, heavy chain 7, cardiac muscle, beta (ßMHC)
CAGCCTACCTCATGGGACTGA
GTGACATACTCGTTGCCCACTTT
6-FAM-TTGTGCCACCCTCGAGT-MGB
NM_017240

NADH dehydrogenase (ubiquinone) 1 alpha subcomplex 10 (Ndufa10)
GGATGATCGGACCTTTCACA
GACGGTCGTGTAATTCAGCA
#89 *
NM_199495

Natriuretic peptide precursor type A (NPPA)
CAACACAGATCTGATGGATTTCA
CGCTTCATCGGTCTGCTC
#25 *
NM_012612

Nuclear respiratory factor 1 (NRF1)
GAAGATCAGCAGACACAAACTCA
TGCCCCAGTACCAACCTG
#77 *
NM_001100708

Nuclear respiratory factor 2 alpha (NRF2a)
TCCAGCATCAGTGCCTTCTG
TAGCTGCCTTTGCGCTACTGT
6-FAM-TACGCCGACTACTATTAAG-MGB
NM_001108841

Peroxisome proliferative activated receptor, gamma, coactivator 1 alpha (PGC-1α)
CTGCGGGATGATGGAGACA
GCGAAAGCGTCACAGGTGTAA
6-FAM-CTATGGTTTCATCACCTACC-MGB
NM_031347.1

Peroxisome proliferator activated receptor alpha (PPAR-α)
TGGAGTCCACGCATGTGAAG
CGCCAGCTTTAGCCGAATAG
6-FAM-CTGCAAGGGCTTCTTTCGGCGA
NM_013196

Peroxisome proliferator-activated receptor gamma, coactivator 1 beta (PGC-1ß)
GCCCTGATGATTCCGAGTTC
TTGGTAAGCGCAGCCAAGA
6-FAM-TGACAGTGAGAATGAAGCTTA-MGB
NM_176075

Polymerase (RNA) II (DNA directed) polypeptide A (Polr2a)
CCAAGTTCAACCAAGCCATT
AGAGACTGAGCAGCCAAAGC
#80 *
XM_001079162

Pyruvate dehydrogenase E1a alpha subunit (PDHE1α)
TGGTCGAGGTAGGTGAGAGCAT
TGGGGTGCACGAGAAGCT
6-FAM-CTCCACGTGCACTGG-MGB
U44125

Pyruvate Dehydrogenase Kinase 4 (PDK4)
CCAACTGCGATGTGGTAGCA
CTGATCGCAGAGCATCTTTGC
6-FAM-TAGTCGAAGATGCCTTTGA-MGB
NM_053551

Pyruvate dehydrogenase phosphatase isoenzyme 1 (PDP1)
ACAGCAGCGGGTGCTCTACT
GAACAGTGGTAGACTGGATGTTCTGA
6-FAM-TGCCCGGAATCC-MGB
AF062740

Ribosomal protein S29 (S29)
CAAGATGGGTCACCAGCAG
CAGACCGTGGCGGTTAGA
#109 *
BC058150

Solute carrier family 2 (facilitated glucose transporter), member 1 (GLUT1)
CATCGTCGTTGGGATCCTTA
GAGCAGTAGAGGCCACAAGTCT
6-FAM-AGGTGTTCGGCTTAGACTCCATCATGG-MGB
BC061873

Solute carrier family 2 (facilitated glucose transporter), member 4 (GLUT4)
CATTCTCGGACGGTTCCTCAT
GGCGATTTCTCCCACATACATA
6-FAM-CGCCTACTCAGGGCTAACATCAGGGTTG-MGB
BC085757

Succinate dehydrogenase complex, subunit B, iron sulfur (Ip) (Sdhb)
CCAAGGGTCTGAATCCAGGAA

TCTCCTTGTAGGTCGCCATCA
6-FAM-CAATTGCAGAAATCAA-MGB
NM_001100539

Transcription factor A, mitochondrial (TFAm))
TGATAGAATTCGTTATGACAATGAAATGA
AGATCACTTCGCCCAACTTCAG
6-FAM-TCTTGGGAAGAGCAAAT-MGB
BC062022

Ubiquinol cytochrome c reductase core protein 2 (Uqcrc2)
AAGATCACCCGTGGAATTGA
TTCCCTTGTTGCAGTCACAC
#119 *
NM_001006970

---

* probe number, "Universal ProbeLibrary Set. Rat" (Roche Applied Science, Mannheim, Germany)

Primers were designed using Primer Express 1.5 (Applied Biosystems, Foster City, CA) and the WWW interface www.universalprobelibrary.com with default settings. To avoid non-specific amplifications, primer sequences were blasted against rat genes. Gel analysis of the PCR products was performed for all sets of primers/probes to ensure single product amplification.

References

1. Lelliott CJ, Medina-Gomez G, Petrovic N, Kis A, Feldmann HM, Bjursell M, Parker N, Curtis K, Campbell M, Hu P, Zhang D, Litwin SE, Zaha VG, Fountain KT, Boudina S, Jimenez-Linan M, Blount M, Lopez M, Meirhaeghe A, Bohlooly YM, Storlien L, Stromstedt M, Snaith M, Oresic M, Abel ED, Cannon B, Vidal-Puig A. Ablation of pgc-1beta results in defective mitochondrial activity, thermogenesis, hepatic function, and cardiac performance. *PLoS biology*. 2006;4:e369
2. Hu P, Zhang D, Swenson L, Chakrabarti G, Abel ED, Litwin SE. Minimally invasive aortic banding in mice: Effects of altered cardiomyocyte insulin signaling during pressure overload. *Am J Physiol Heart Circ Physiol*. 2003;285:H1261-1269
3. Schaeffer PJ, Desantiago J, Yang J, Flagg TP, Kovacs A, Weinheimer CJ, Courtois M, Leone TC, Nichols CG, Bers DM, Kelly DP. Impaired contractile function and calcium handling in hearts of cardiac-specific calcineurin b1-deficient mice. *Am J Physiol Heart Circ Physiol*. 2009;297:H1263-1273
4. Baumgarten G, Knuefermann P, Kalra D, Gao F, Taffet GE, Michael L, Blackshear PJ, Carballo E, Sivasubramanian N, Mann DL. Load-dependent and -independent regulation of proinflammatory cytokine and cytokine receptor gene expression in the adult mammalian heart. *Circulation*. 2002;105:2192-2197
5. Belke DD, Betuing S, Tuttle MJ, Graveleau C, Young ME, Pham M, Zhang D, Cooksey RC, McClain DA, Litwin SE, Taegtmeyer H, Severson D, Kahn CR, Abel ED. Insulin signaling coordinately regulates cardiac size, metabolism, and contractile protein isoform expression. *J Clin Invest*. 2002;109:629-639
6. Litwin SE, Zhang D, Roberge P, Pennock GD. Ditpa prevents the blunted contraction-frequency relationship in myocytes from infarcted hearts. *American journal of physiology*. 2000;278:H862-870
7. Veksler VI, Kuznetsov AV, Sharov VG, Kapelko VI, Saks VA. Mitochondrial respiratory parameters in cardiac tissue: A novel method of assessment by using saponin-skinned fibers. *Biochim Biophys Acta*. 1987;892:191-196
8. Mazumder PK, O'Neill BT, Roberts MW, Buchanan J, Yun UJ, Cooksey RC, Boudina S, Abel ED. Impaired cardiac efficiency and increased fatty acid oxidation in insulin-resistant ob/ob mouse hearts. *Diabetes*. 2004;53:2366-2374
9. Suga H. Ventricular energetics. *Physiological reviews*. 1990;70:247-277
10. Kim HJ, Kim KW, Yu BP, Chung HY. The effect of age on cyclooxygenase-2 gene expression: Nf-kappab activation and ikappabalpha degradation. *Free radical biology & medicine*. 2000;28:683-692
11. O'Neill BT, Kim J, Wende AR, Theobald HA, Tuinei J, Buchanan J, Guo A, Zaha VG, Davis DK, Schell JC, Boudina S, Wayment B, Litwin SE, Shioi T, Izumo S, Birnbaum MJ, Abel ED. A conserved role for phosphatidylinositol 3-kinase but not akt signaling in mitochondrial adaptations that accompany physiological cardiac hypertrophy. *Cell Metab*. 2007;6:294-306
12. Weibel E. Steriological principles for morphometry in electron microscopic cytology. *Int Rev Cytol*. 1979;26:235-302